

## Article

# Non-Invasive Assessment of Water-Based Gel Cleaning on a Capogrossi Oil Painting Using NMR-MOUSE

Noemi Proietti <sup>1</sup>, Patrizia Moretti <sup>2,†</sup>, Eleonora Maniccia <sup>3</sup>, Paola Carnazza <sup>4</sup>, Daphne De Luca <sup>5</sup>, Costanza Miliani <sup>6</sup> and Valeria Di Tullio <sup>1,\*</sup>

<sup>1</sup> Institute of Heritage Science (CNR-ISPC), National Council of Research, 00016 Montelibretti, Italy

<sup>2</sup> Institute of Chemical Sciences and Technologies “Giulio Natta”, (CNR-SCITEC), National Council of Research, 06123 Perugia, Italy

<sup>3</sup> Department of Physics and Chemistry-Emilio Segré (DiFC), University of Palermo, 90100 Palermo, Italy

<sup>4</sup> Galleria Nazionale d’Arte Moderna e Contemporanea, 00197 Roma, Italy

<sup>5</sup> Department of Pure and Applied Sciences (DiSPeA), University of Urbino Carlo Bo, 61029 Urbino, Italy

<sup>6</sup> Institute of Heritage Science (CNR-ISPC), National Council of Research, 80134 Naples, Italy

\* Correspondence: valeria.ditullio@cnr.it

† Current address: Department of Environment, Constructions and Design (DACD), University of Applied Sciences and Arts of Southern Switzerland (SUPSI), Via Flora Ruchat Roncati 15, 6850 Mendrisio, Switzerland.

## Abstract

This study investigates water-based gel and gel-like cleaning treatments on *Superficie 553*, an oil painting on canvas by Giuseppe Capogrossi, using portable NMR to assess their impact. The objective was to evaluate the effects of four cleaning systems composed of a buffer solution released in free form and combined with xanthan gum, a cross-linked silicone polymer gel, and an agar gel matrix. Two distinct NMR experiments were conducted. The first involved the acquisition of <sup>1</sup>H depth profiles to detect the distribution of the cleaning solution within the painted layer and the thickness variations resulting from cleaning procedures. The second employed the acquisition of relaxation times, facilitating the investigation of molecular mobility within the organic components of the paint layer. NMR results indicated that the agar gel system caused negligible structural changes, whereas the silicone gel induced rigidification, and the other systems permanently increased molecular mobility. These measurements provided insights into alterations in the dynamic behavior of the polymerized oil. A key strength of this investigation lies in the direct application of diagnostic methods on *Superficie 553*, made possible by the non-invasive nature and portability of the NMR-MOUSE system. Additionally, portable FTIR was used to detect residues and obtain chemical information, confirming that the silicone gel left detectable residues and identifying the agar gel as the most conservative cleaning method. This enabled in situ analysis of the original artwork without sampling or relocation—a crucial advantage given the difficulty of replicating the complex physicochemical conditions of historical paint surfaces under laboratory constraints. Such real-time, on-site monitoring ensured an authentic evaluation of the treatment effects, preserving the integrity of the artwork throughout the conservation process.

**Keywords:** oil painting; NMR; gel; cleaning; molecular dynamic

Academic Editor: Magali Brunet

Received: 1 November 2025

Revised: 19 December 2025

Accepted: 12 January 2026

Published: 15 January 2026

**Copyright:** © 2026 by the authors. Licensee MDPI, Basel, Switzerland. This article is an open access article distributed under the terms and conditions of the [Creative Commons Attribution \(CC BY\) license](https://creativecommons.org/licenses/by/4.0/).

## 1. Introduction

The conservation of easel paintings represents a significant challenge within the field of cultural heritage preservation, with cleaning being one of the most delicate and irreversible interventions. While traditional paintings have been extensively studied, artworks created from the 19th century onwards present a distinct set of complexities. The industrial revolution introduced a vast array of new materials, leading artists to use commercially prepared tube paints containing complex mixtures of synthetic pigments, binders, and additives such as extenders, driers, and stabilizers. This shift resulted in paint films that are highly heterogeneous and whose chemical and physical properties are often poorly understood. Furthermore, a significant stylistic shift occurred during this period, with many artists opting to leave their works unvarnished to achieve specific matte effects; this absence of a protective varnish layer exposes the original paint film directly to environmental agents and conservation treatments.

This material complexity makes the response of modern paint films to conservation treatments, particularly aqueous cleaning methods, highly unpredictable. The cleaning of such unvarnished surfaces is especially critical because, unlike traditional artworks where the varnish acts as a sacrificial barrier, the cleaning agents interact directly with the sensitive pictorial layer. The interaction of water and organic solvents with these composite systems can induce a range of deleterious effects, including pigment leaching, binder swelling, surfactant mobilization, and surface blanching.

Water sensitivity in oil paintings is related to several factors that can be directly linked to the artist's technique (for example, the formation of lean paint films where the pigments are not well-bound to each other or to the medium) or the material's composition. Regarding the material's composition, its sensitivity to water derives mainly from the type of pigment used, but also, as has emerged in recent years, from the presence of additives incorporated into the paint tube, which modify the molecular composition of the oil paint film and, in turn, influence its sensitivity to water [1,2]. It has also been demonstrated that the primary cause of an oil film's sensitivity to water is the conversion of magnesium carbonate, often used as an extender, into magnesium sulfate heptahydrate (Epsomite) [3,4]. This water-soluble compound forms following the artwork's exposure to sulfur dioxide, one of the main pollutants present in the air.

Another important water-driven degradation process is the activation of metal soaps, which compromises the structural and aesthetic integrity of a paint film [5–7]. This problem is particularly complex in 20th-century works, where metal soaps have a dual origin. They can form *in situ* through degradation reactions between pigments like zinc white (ZnO) and free fatty acids from the oil binder, but they are also frequently present from the moment of creation as intentional additives (e.g., zinc or aluminum stearates) used by manufacturers to control the paint's properties [8]. Whether formed through degradation or included as an additive, metal soaps are mobile species within the paint matrix [9,10]. The presence of water has been identified as a critical factor that activates their degradation pathways. Exposure to moisture acts as a plasticizer for the paint matrix, increasing the mobility of these pre-existing compounds. This allows them to migrate, aggregate, and precipitate in a crystalline form. This process can generate significant internal stresses, leading not only to surface efflorescence but also to the formation of damaging protrusions and delamination within the paint structure [11].

This inherent sensitivity to moisture raises critical questions regarding conservation practices, particularly the use of aqueous cleaning systems. The application of aqueous treatments, therefore, poses a significant and potentially underestimated risk of triggering the migration and crystallization of these additives, leading to irreversible structural and visual damage.

By examining the case of *Superficie 553*, a painting confirmed to contain zinc soaps [12], this study aimed to identify a cleaning system that provides the optimal balance between maximum cleaning efficacy and minimal alteration of the painting's physicochemical properties due to water. Furthermore, the cleaning of *Superficie 553* is an exceptionally delicate operation. In such a sensitive case, the use of gels or gelling agents is essential to precisely control the release of the cleaning solution, thereby minimizing its penetration into the porous paint layer and preventing potential damage [13–15].

In this study, a buffer solution incorporated into different aqueous-based cleaning formulations, specifically based on xanthan gum, a silicone polymer rubbery gel, and agarose gel, was studied, combined with an aspiration system to minimize water contact on the unvarnished paint surface. All these systems were selected to reduce the contact time between the cleaning solution and the painting surface. They have fundamentally different chemical structures and physical properties. VelvesilPlus® is a gel-like silicone polyether copolymer that was adopted to create stable emulsions in a silicone solvent continuous phase. It is an organogel, meaning its primary structure is non-aqueous. When an aqueous cleaning solution is added, it creates a stable water-in-silicone emulsion. This class of substances is very useful when working on surfaces that are highly sensitive to water, such as acrylics, which, being composed of many surfactants and additives, could experience leaching phenomena when water is used, resulting in increased porosity and fragility of the paint film [16–18]. Xanthan gum (Vanzan NF-C®) is a natural polysaccharide produced by bacterial fermentation. It is used to create hydrogels and has been used in the cleaning of oil paintings, metal, and lapideous objects [19–21]. Agar-agar gel is now one of the most studied hydrogels in the field of art conservation. Agar is a complex polysaccharide derived from red algae. It is composed of two main components: agarose, a neutral, linear polymer, and agarpectin, a more complex, branched, and sulfated polymer. The gelling property of agar is primarily due to the agarose component, which forms a porous, three-dimensional network that can hold a significant amount of water. It is used in very different scenarios, from cleaning stone materials to bio-cleaning, and has been applied to water-sensitive paintings. It has shown excellent properties in both releasing and controlling the delivery of water and solvents [22–30].

To characterize the behavior of the gel cleaning systems, Nuclear Magnetic Resonance (NMR) was applied directly on the paintings during the preliminary tests performed by the restorer. NMR spectroscopy, particularly the measurement of relaxation times, has emerged as a uniquely powerful, non-invasive tool for this purpose. Unlike techniques that primarily provide elemental or molecular composition, NMR relaxometry is sensitive to molecular dynamics—the rotational and translational motion of molecules on a nanoscopic scale. This dynamic information serves as a direct and sensitive proxy for the material's physical state, such as its viscosity, rigidity, and degree of polymerization [31–34].

NMR-MOUSE is an advanced portable tool that applies a magnetic field to one side of the object, allowing measurements of the object without sampling and in a fully preserved way [35,36]. Because of the ability to measure the hydrogen content as a function of depth of measurement [37,38], NMR is a very powerful technique to evaluate information on the structure and thickness of hydrogen-rich layers, information that is very useful in the conservation of paintings. This capability can also be exploited for monitoring the physicochemical properties of paintings [39–41] and evaluating the diffusion of water and organic solvents and the pictorial layer changes due to the interaction with these compounds [42–45]. Moreover, because the reduction in the thickness of layers under removal is strictly correlated with the power of the cleaning system, hydrogen depth profiles collected by unilateral NMR on the surface of the painting before and after the cleaning treatment can be used to evaluate the physicochemical effects of the cleaning system applied [46].

In addition to evaluating the presence of the cleaning system residues, portable External Reflection Fourier Transform Infrared Spectroscopy (ER-FTIR) analyses were conducted both before and after the cleaning tests [47,48]. This technique is particularly suitable for assessing delicate, unvarnished surfaces, as it allows for the non-contact identification of functional groups. While NMR provides physical data regarding the painting's rigidity and swelling, ER-FTIR offers complementary chemical information, allowing for the specific detection of potential residues from the cleaning agents—such as silicone or polysaccharides—and ensuring they are distinguished from the original paint binder. The presence of cleaning residues requires particular attention, especially in unvarnished paintings. Since these residues can migrate into the paint layers, they can, over time, trigger yellowing, alter the visual appearance of the artwork, and activate further degradation processes affecting the painting's original materials.

The application of integrated analytical techniques in the monitoring of cleaning systems provided valuable insights into their specific behavior and effectiveness when applied in situ on painting surfaces.

## 2. Materials and Methods

### 2.1. Case Study

The artwork under investigation is *Superficie 553*, painted by the Italian master Giuseppe Capogrossi (1900–1972) and currently conserved at the National Gallery of Modern and Contemporary Art in Rome (Figure 1a). Created in 1965, this painting represents the mature phase of the artist's most famous period (the *Informal* period), characterized by his obsessive and rhythmic repetition of a single, enigmatic symbol, often referred to as “fork” or “tetradent”. The support of the painting consists of a single piece of plain-weave cotton canvas. As reported by a study performed by La Nasa et al. [12], the painting was created with two distinct preparatory layers. The initial industrial ground is a complex mixture of animal glue, a siccative oil, and egg yolk, with Zinc White used as a filler. Over this ground, the artist applied a second priming layer composed of a siccative oil binder pigmented with Zinc White. The black ideograms are painted with a mixture of Ivory Black and Prussian Blue, which also contains cobalt as a siccative additive. The red paint consists of Cadmium Red, with barium present as an extender. The final white background is a mixture of Titanium White and Zinc White in a siccative oil binder. In addition to the primary pigments and binders, wax was found within the black and red paint areas. Furthermore, zinc oxalates and carboxylates (metal soaps) are present throughout the paint layers, indicating their use as industrial additives in the commercial paints used by the artist; however, this finding does not preclude their concurrent formation as degradation products resulting from the interaction between the oil binder and zinc ions present in the preparatory and pictorial layers as well.

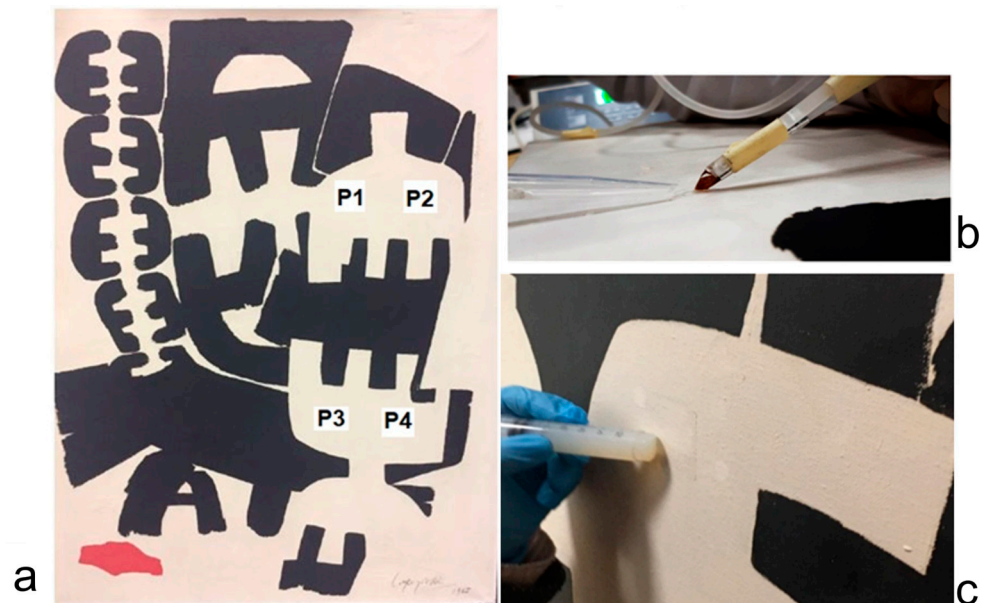


**Figure 1.** (a) Painting *Superficie 553*, with areas P1–P4 monitored using portable NMR before and after cleaning (approximate area size  $5 \times 5$  cm); (b) Application of the cleaning system: buffer solution released by a syringe pump and immediately removed by a micro-aspirator; (c) Application of the agar stick on area P3 (bottom).

## 2.2. Cleaning Tests

Considering the unvarnished nature of the paint and the presence of metal soaps, the risk of swelling was managed by strictly limiting the contact time. Based on preliminary cleaning tests, three water-based gels were selected: xanthan gum (Vanzan NF-C<sup>®</sup>, CTS, Altavilla Vicentina (VI), Italy), a naturally derived polymer produced by the bacterium *Xanthomonas campestris*, which consists of a main cellulose chain where side chains made of three simple sugars (an acidic trisaccharide chain) are attached to each glucose ring; a cross-linked silicone polymer (VesvelilPlus<sup>®</sup>, Bresciani srl, Milan, Italy) that can form a soft, pliable gel; and a rigid agarose gel (Sigma-Aldrich, Merck KGaA, Darmstadt, Germany). A buffer solution at pH 5.6 was prepared using acetic acid and sodium hydroxide as the base solution for the four types of cleaning systems.

Four white paint regions (labeled P1–P4), covered by a yellowed layer likely caused by the deposition of smoke dust, were selected for testing. These areas correspond to the white background paint composed of Titanium and Zinc White in safflower oil [12]. The layer to be removed is very thin; it is hypothesized that it cannot be detected by NMR, as its thickness is presumably below the instrument's  $40 \mu\text{m}$  spatial resolution. The cleaning operations were performed by the restorer with a strictly controlled contact time of 1–2 min to minimize interaction. The treatment protocols were as follows: P1 area was cleaned using the buffer solution released by a syringe pump (Graseby, MDKMed Medical Technology Co., Ltd., Hangzhou, China) combined with a micro-aspirator (3A Health Care srl, Lonato del Garda, Italy) (see Figure 1b); Area P2 was treated with an emulsion containing 10% buffer solution in a silicone polymer gel (VesvelilPlus<sup>®</sup>) (pH 5.6, conductivity 3.3 mS/cm), released by a syringe pump combined with a micro-aspirator and cleared gently with the non-polar silicone solvent D5 (decamethyl-cyclopenta-siloxane), (CTS, Altavilla Vicentina (VI), Italy); Area P3 was treated with an agar stick (2% *w/w*) prepared with the buffer solution (pH 5.6, conductivity 3.2 mS/cm, containing 2% Agar) (see Figure 1c); and Area P4 was treated with the buffer solution (pH 5.6, conductivity 3.2 mS/cm) thickened

with 2.9% xanthan-gum gel (Vanzan NF-C®) applied with a syringe pump and removed with a micro-aspirator.

### 2.3. NMR-MOUSE

<sup>1</sup>H depth profiles and transverse relaxation times were acquired at 13.62 MHz using a portable Bruker Biospin NMR instrument (Bruker Corporation, Billerica, MA, USA) interfaced with a single-sided sensor from RWTH Aachen University, which generates a highly uniform magnetic field gradient (14 T m<sup>-1</sup>) to resolve near-surface structures. Depth profiles were obtained by repositioning the sensor in 70 μm increments across the painting. The experimental conditions to acquire the <sup>1</sup>H profiles were echo time 41 μs, relaxation delay 0.6 s, 32 scans, rf pulse 5.5 μs, and a nominal resolution of 40 μm.

To ensure the <sup>1</sup>H depth profile was exclusively dependent on proton spin density, the intensity of each experimental point was calculated from the average of the first three echoes. At the interface between the pictorial layer and the canvas layer (around 200 μm), transverse relaxation times (T<sub>2</sub>) were measured using a CPMG sequence with an echo time of 41 μs, 2048 scans, relaxation delay of 2 s, 512 echoes, and a resolution of 200 μm. The resulting experimental data were analyzed using an Inverse Laplace Transformation (ILT) algorithm via the UPEN-MATLAB routine, where W<sub>i</sub> is the spin population, and T<sub>2i</sub> is the transverse relaxation time of the *i*th component.

*Superficie 553* was subjected to two phases of NMR analysis. During the first phase, the paint material was investigated to obtain information about the thickness of its constituent layers in four different areas of the painting. The second phase was carried out immediately after the cleaning process to monitor the state of the painting. It is important to note that the transient swelling occurring during the cleaning action was not monitored due to the operational constraints of performing in situ analysis, which prevents the sensor from being positioned simultaneously with the cleaning tool. Furthermore, the rapid kinetics of the initial swelling phase (occurring within the 1–2 min application window) cannot be resolved by the acquisition time required for depth profiling. Therefore, the aim of the NMR monitoring was not to observe the transient swelling peak but to evaluate the long-term behavior of the painting by detecting permanent, irreversible alterations (such as binder leaching or rigidification) remaining after solvent evaporation.

### 2.4. ER-FTIR

External reflection FTIR (ER-FTIR) analyses were performed using a portable Bruker Optics ALPHA spectrometer, equipped with a SiC global infrared source and a DLaTGS detector (Bruker Corporation, Billerica, MA, USA). A system of parabolic mirrors directs and collects (at a 22°/22° angle) the infrared radiation reflected from the surface positioned at a working distance of about 1 cm, within a spectral range from 7500 cm<sup>-1</sup> to 350 cm<sup>-1</sup>. The diameter of the analyzed spot was approximately 4 mm, and the spectral resolution was set to 4 cm<sup>-1</sup>.

## 3. Results

### 3.1. NMR-MOUSE Analysis

NMR analysis was carried out before and after cleaning, followed by a third phase of measurements taken seven days after the application of each method. The results from these analyses are presented in Figure 2a–d.

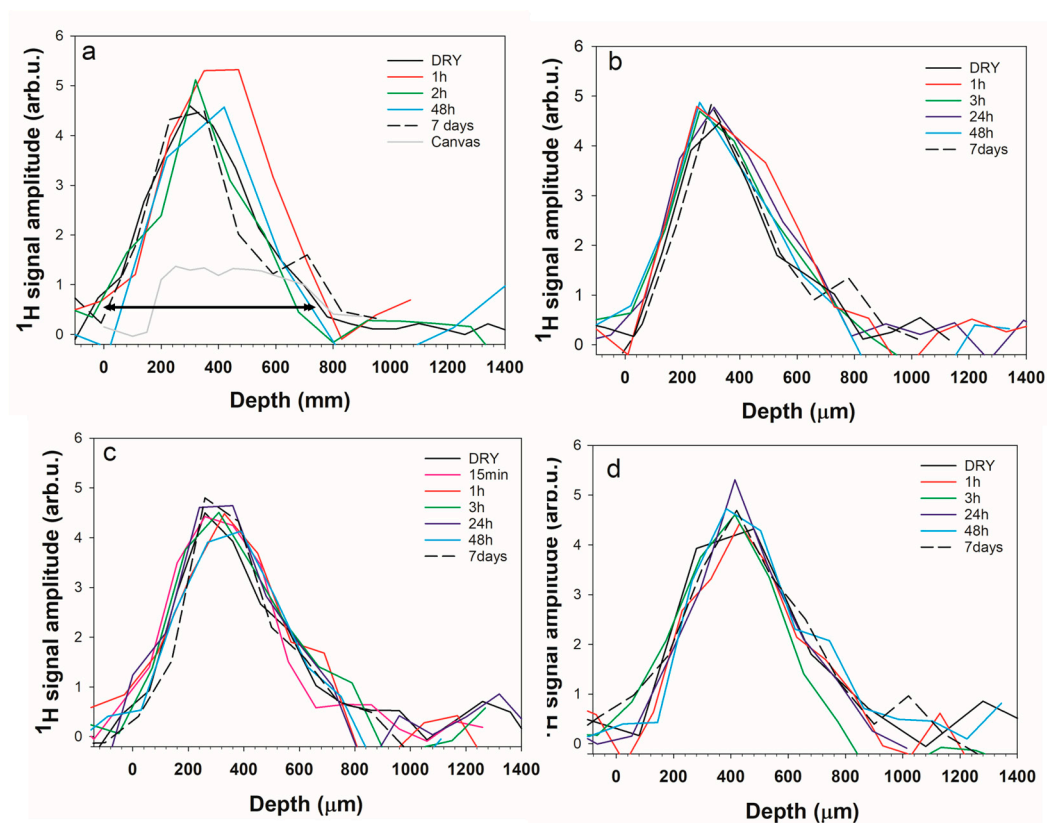


**Figure 2.**  $^1\text{H}$  NMR profiles obtained on areas P1, P2, P3 and P4 of painting *Superficie 553* before cleaning (dry) and after 1 h, 2–3 h, 12 h, 24 h, 48 h and 7 days. (a) P1 treated with buffer solution (BS); (b) P2 treated with BS emulsified in VelvesilPlus<sup>®</sup>; (c) P3 treated with BS in an agar stick; and (d) P4 treated with BS thickened with Vanzan NF-C<sup>®</sup>.

From the results obtained before cleaning, a high degree of homogeneity was found in the thickness of the four test areas, with a recorded average thickness of approximately 600  $\mu\text{m}$ , including the canvas support. To differentiate the hydrogen signal contributions of the canvas and the pictorial layer, an unpainted section of the canvas was analyzed (see Figure 2a, grey line). The results showed that the canvas itself was approximately 500  $\mu\text{m}$  thick; by subtraction, the thickness of the pictorial layer was determined to be approximately 100  $\mu\text{m}$ .

Furthermore, the  $^1\text{H}$  profile revealed that the pictorial layer is not a distinct layer separate from the canvas. Instead, the oil binder appears to have been absorbed into the canvas weave. This resulted in an increased hydrogen signal distributed throughout the entire thickness of the sample, rather than being confined to the upper 100  $\mu\text{m}$ .

In area P1, the NMR profile obtained one hour after the application of the free buffer solution showed a slight increase in the  $^1\text{H}$  signal, indicating the presence of the solution within the paint layer. At this stage, an increase of about 150  $\mu\text{m}$  in the painting's thickness was observed (see Figure 2a). However, after 2 h, the swelling decreased, and on the seventh day, the deviation from the initial  $^1\text{H}$  profile was negligible, confirming a return to the initial state. A similar increase was observed at point P2, 48 h after the application of the cleaning treatment. In both cases, after seven days, the thickness of the painting returned to the value observed before cleaning.

The profiles of the other points show less evident swelling, and in general, after seven days, the recorded profiles are consistent with those acquired before cleaning. At longer time intervals, the NMR profiles for all treated areas showed no significant variations in the thickness of the paint layer following the cleaning. Area P3 proved to be the most stable zone, both at short times (approximately 1 h after cleaning) and after 7 days.

To investigate the molecular dynamics, specific measurements of the transverse relaxation time ( $T_2$ ) were performed on the pictorial layer. Before interpreting the results, it is essential to explain the type of information that can be obtained by measuring the  $T_2$ . The transverse relaxation time is an important NMR parameter that depends on numerous factors related to the time scale of molecular motions. In the case of oil paintings,  $T_2$  values are correlated with the degree of cross-linking, the degree of hydrolysis, and the molecular weight of the oil binder components, and therefore with their viscoelastic and rigidity properties [35,39,40].

In the case of *Superficie 553*, the selected areas (P1–P4) showed subtle differences in their  $T_2$  values prior to cleaning (see Figure 3a,b).

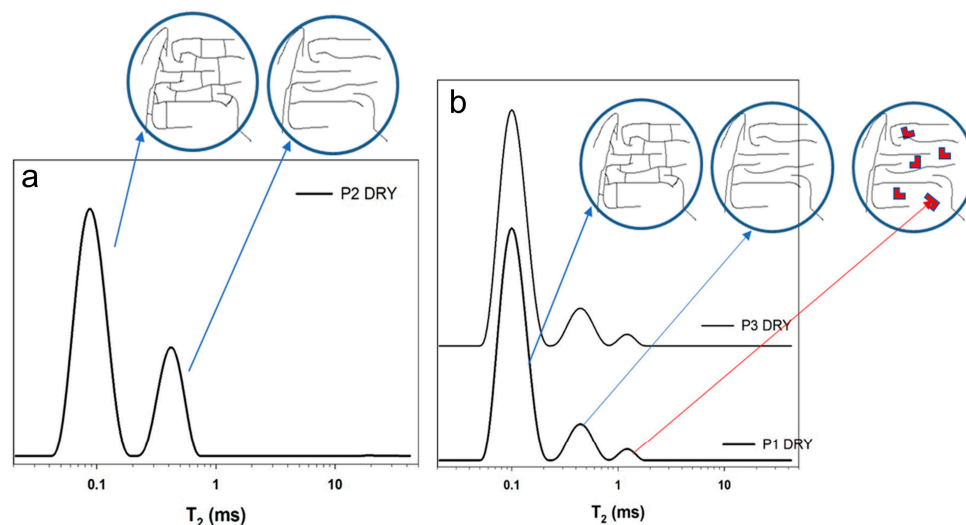


**Figure 3.** (a)  $T_2$  distributions obtained on area P2; (b)  $T_2$  distributions obtained on P1 and P3 areas.

Figure 3a displays the distribution of  $T_2$  relaxation times characterizing the paint layer at point P2. The graph reveals two primary values: one at approximately 0.1 ms and the other around 0.6 ms. The presence of two relaxation times is explained by the existence of two domains distinguished by the different mobility (molecular motion) of hydrogen in the polymerized oil matrix. The shorter component,  $T_{2a}$  (0.1 ms), is attributed to hydrogen nuclei in molecules with reduced motion because they are cross-linked (indicating a higher degree of oil polymerization). The longer component,  $T_{2b}$  (0.5–0.6 ms), on the other hand, relates to hydrogens with greater mobility within the polymeric network (such as hydrogens in saturated aliphatic chains). The presence of two distinct relaxation times is characteristic of polymerized oil and has been previously found in other paintings [35,40]. The area of each peak indicates the relative population of hydrogens in each domain. In this case, almost 80% of the hydrogens arise from the rigid cross-linked matrix, and 17–20% correspond to the higher mobility state of the aliphatic chains. A small third relaxation component,  $T_{2c}$  approximately 1–2 ms, was also observed, similar to P1 and P3 (see Figure 3b). This component accounts for roughly 3% of the total hydrogen signal and can be attributed to the presence of low molecular weight molecules that exhibit higher mobility. Its origin could be due to the presence of low molecular weight species or minor degradation products that are more mobile.

Following the cleaning procedure, the P1 area (treated with the buffer solution applied with the syringe pump) exhibited significant variation in molecular mobility over a period of seven days, see Figure 4a. Initially, in the dry state, the surface was characterized by three distinct molecular populations: a dominant, highly rigid component ( $T_{2a}$ ) making up 85% of the signal with a very short value of 0.10 ms; a smaller semi-mobile component ( $T_{2b}$ ) at 12% with a value of 0.5 ms; and a minor highly mobile component ( $T_{2c}$ ) at 3% with

a value of 1.2 ms. The immediate impact of the cleaning solution, visible three hours after application, was a plasticizing effect. The absorption of the buffer solution into the polymer matrix dramatically increased the molecular mobility. This was most evident in the highly mobile  $T_{2c}$  component, whose  $T_2$  value increased to 5 ms, likely representing the liquid cleaner itself trapped within the surface. This molecular-level softening corresponds directly to the physical swelling of the paint layer, correlating with what was observed in the  $^1\text{H}$  profile at this early stage.

Over the subsequent days, as the solution evaporated, the surface began to recover. By 24 h, the  $T_2$  values had largely decreased towards their original levels. However, between 48 and 66 h, the main rigid component,  $T_{2a}$ , became even more rigid than it was initially, with its  $T_2$  value dropping to a low of 0.07 ms. This suggests a transient state of increased rigidity, possibly caused by the leaching of some naturally present mobile molecules by the cleaning solution, causing the remaining polymer network to contract and become more constrained as it dries. A critical observation was made at the seven-day mark. While the physical swelling had completely subsided and the painting's thickness had returned to its initial state, the NMR relaxation data revealed that a structural change had occurred at the molecular level. The system did not revert to its original molecular distribution. Instead, a significant portion of the most rigid component converted into a more flexible state. The population of the rigid component decreased from 85% to 74%, while the population of the semi-mobile component nearly doubled, rising from 12% to 23% (see Table 1). This behavior can be explained by the hypothesis that the cleaning process mobilizes lower molecular weight species within the polymer matrix.

**Table 1.**  $T_2$  values of areas P1, P2, P3, and P4 (obtained by fitting the  $T_2$  relaxation decays using the UPEN algorithm), before (dry) and after the cleaning procedure.

<b>P1 Buffer Solution + Syringe Pump</b>						
<b>Time (hours)</b>	<b><math>W_a</math></b>	<b><math>T_{2a}</math></b>	<b><math>W_b</math></b>	<b><math>T_{2b}</math></b>	<b><math>W_c</math></b>	<b><math>T_{2c}</math></b>
DRY	85%	0.10	12%	0.5	3%	1.2
3 h	89%	0.12	10%	0.7	1%	5
24 h	86%	0.10	13%	0.5	<1%	1.5
48 h	82%	0.08	18%	0.5	-	-
66 h	87%	0.07	12%	0.6	<0.5%	1.8
7 d	74%	0.10	23%	0.4	3%	1.5
<b>P2 VelvesilPlus®</b>						
<b>Time (hours)</b>	<b><math>W_a</math></b>	<b><math>T_{2a}</math></b>	<b><math>W_b</math></b>	<b><math>T_{2b}</math></b>	<b><math>W_c</math></b>	<b><math>T_{2c}</math></b>
DRY	74%	0.09	26%	0.4	-	-
3 h	84%	0.1	15%	0.5	1%	3.0
24 h	84%	0.1	14%	0.4	2%	0.7
48 h	89%	0.1	11%	0.5	-	-
7 d	80%	0.09	18%	0.40	2%	2
<b>P3 Agar</b>						
<b>Time (hours)</b>	<b><math>W_a</math></b>	<b><math>T_{2a}</math></b>	<b><math>W_b</math></b>	<b><math>T_{2b}</math></b>	<b><math>W_c</math></b>	<b><math>T_{2c}</math></b>
DRY	85%	0.10	12%	0.47	3%	1
3 h	87%	0.11	12%	0.54	1%	1.6
24 h	81%	0.10	18%	0.50	1%	5
48 h	87%	0.12	11%	0.60	2%	2
7 d	80%	0.09	18%	0.40	2%	2
<b>P4 Vanzan NF-C®</b>						
<b>Time (hours)</b>	<b><math>W_a</math></b>	<b><math>T_{2a}</math></b>	<b><math>W_b</math></b>	<b><math>T_{2b}</math></b>	<b><math>W_c</math></b>	<b><math>T_{2c}</math></b>
DRY	86%	0.12	14%	0.7	-	-
3 h	81%	0.10	19%	0.6	-	-

24 h	74%	0.10	25%	0.4	1%	7
96 h	84%	0.10	14%	0.5	2%	2
7 d	80%	0.10	18%	0.4	2%	1

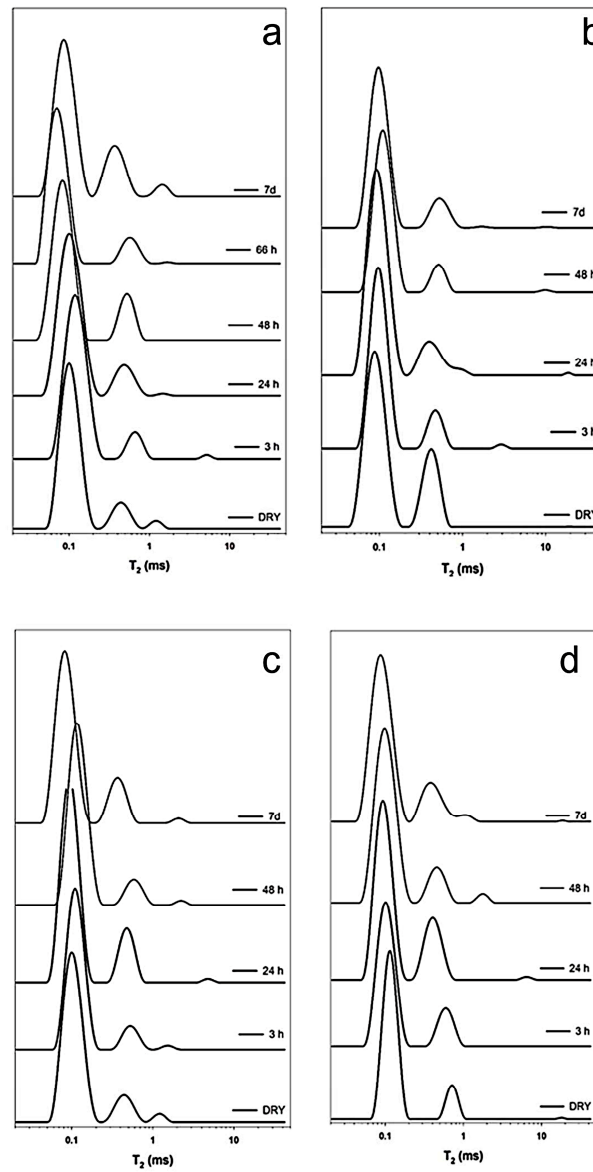


**Figure 4.**  $T_2$  distributions obtained on the white areas (a) P1, (b) P2, (c) P3, and (d) P4, before (DRY) and after 3 h, 24 h, 48 h, 66 h, and 186 h (7 days) of the cleaning procedure.

At point P2, treated with the buffer solution emulsified in the silicone polymer gel (VesvelilPlus®), initially, in its dry state, the paint layer was composed of a rigid polymer matrix (component  $T_{2a}$ ) that accounted for 74% of the hydrogen population, but this was balanced by a significant fraction of a more flexible component ( $T_{2b}$ ) constituting the remaining 26%, see Figure 4b. In contrast, the final state observed seven days after treatment revealed a distinct shift in molecular mobility towards greater rigidity. The rigid component,  $T_{2a}$ , now dominated the system, having increased to encompass 85% of the material, while the mobile fraction,  $T_{2b}$ , significantly diminished, now representing only 15%. This shift represents not a subtle variation but a substantial conversion of approximately 11% of the material from a flexible to a rigid state. This transformation was initiated almost immediately upon application. The transient appearance of a third, highly mobile peak at three hours is attributed to the molecular signature of the VesvelilPlus® gel

itself. More importantly, the data indicate that the underlying redistribution of the painting's components happens quickly and persists.

In area P3, the initial paint layer was composed of a dominant rigid component,  $T_{2a}$  ( $W_a = 85\%$ ), a semi-mobile component,  $T_{2b}$  ( $W_b = 12\%$ ), and a small, highly mobile component,  $T_{2c}$  ( $W_c = 3\%$ ), see Figure 4c. Following treatment using BS in an agar–agar gel stick, three hours after application, the changes were notably limited. The distribution of the molecular populations remained almost identical to the initial state. Only a very slight increase in the  $T_2$  values was observed, indicating a minimal plasticizing effect that can be considered negligible. Over the drying period, minor fluctuations in the component weights were recorded, with a temporary increase in the semi-mobile fraction ( $T_{2b}$ ) at 24 h and again at 7 days. This suggests a slow, dynamic process of solvent evaporation and polymer chain rearrangement. By the seventh day, the system had stabilized to a state extremely close to its original condition. The final composition showed the rigid component ( $T_{2a}$ ) at 80% and the semi-mobile component ( $T_{2b}$ ) at 18%. This represents a very modest conversion (approximately 5%) of the rigid material to a more flexible state. The  $T_2$  relaxation times themselves returned almost exactly to their initial values, confirming that the intrinsic nature of the molecular components remained unaltered.

In area P4, treated with xanthan gum (VanzanNF-C<sup>®</sup>), the untreated paint layer initially exhibited a predominantly rigid molecular architecture, with the primary component ( $T_{2a}$ ) constituting 86% of the material ( $T_2 = 0.12$  ms), complemented by a smaller, semi-mobile fraction of 14% ( $T_{2b} = 0.7$  ms), see Figure 4d. The temporal evolution following the application of the buffer solution in xanthan gum gel revealed a delayed interaction. While a minor initial perturbation was observed at three hours, the most significant effect manifested at 24 h, where the system underwent maximum plasticization. At this stage, the rigid fraction ( $T_{2a}$ ) was substantially reduced to 74%, while the semi-mobile fraction ( $T_{2b}$ ) increased to 25%. Concurrently, a new, highly mobile component ( $T_{2c}$ ) emerged with a very long relaxation time ( $T_2 = 7$  ms). Although this constituted only a small fraction of the signal, its appearance indicated a slight plasticizing effect of water on the polymeric network. However, this effect was less pronounced than that observed in P1, which was treated with the free buffer solution applied via a syringe pump.

### 3.2. ER-FTIR Analysis

The chemical alterations induced by the four cleaning systems were investigated by comparing the ER-FTIR spectra of the treated surfaces with reference data from the untreated areas. ER-FTIR investigations confirmed that no variations in the chemical composition of the paint layer, made of an oil-based mixture of Zinc White and Titanium White, were found in the areas treated with the free buffer solution (P1), the agar gel (P3), and the Xanthan gum gel (P4). Specifically, the FTIR spectra collected from areas P1, P3, and P4 before and after the cleaning tests exhibited a perfect overlap with the characteristic bands of the original paint layer. The key vibrational modes of the oil binder (C=O *stretching* at  $1738\text{ cm}^{-1}$ , C–H *stretching* at  $2920\text{--}2850\text{ cm}^{-1}$ ) and the inorganic components—zinc oxalates ( $1320$  and  $1364\text{ cm}^{-1}$ ), zinc carboxylates ( $1540\text{ cm}^{-1}$ ), and the Titanium/Zinc white pigments—remained unaltered in both intensity and position. In contrast, in area P2, treated with the silicone polymeric emulsion (VelvesilPlus<sup>®</sup>), two additional bands at ca.  $1260$  and  $2960\text{ cm}^{-1}$  attributable to cleaning formulation residues were detected (Figure 5). The first is assigned to the symmetric deformation of the Si-CH<sub>3</sub> group, while the second corresponds to the C–H stretching characteristic of the methyl groups in the silicone polymer chain. These bands appeared at maximum intensity after the dry removal of the gel (Step 1), while after the two rinsing steps with cyclomethicone D5 (Steps 2 and 3), their relative intensity was significantly reduced, but the washing failed to eliminate them completely. Overall, the data obtained from the ER-FTIR monitoring of area P2

highlighted the risk of residue retention from the silicone polymeric emulsion, which poses a potential threat to the long-term conservation of the artwork.

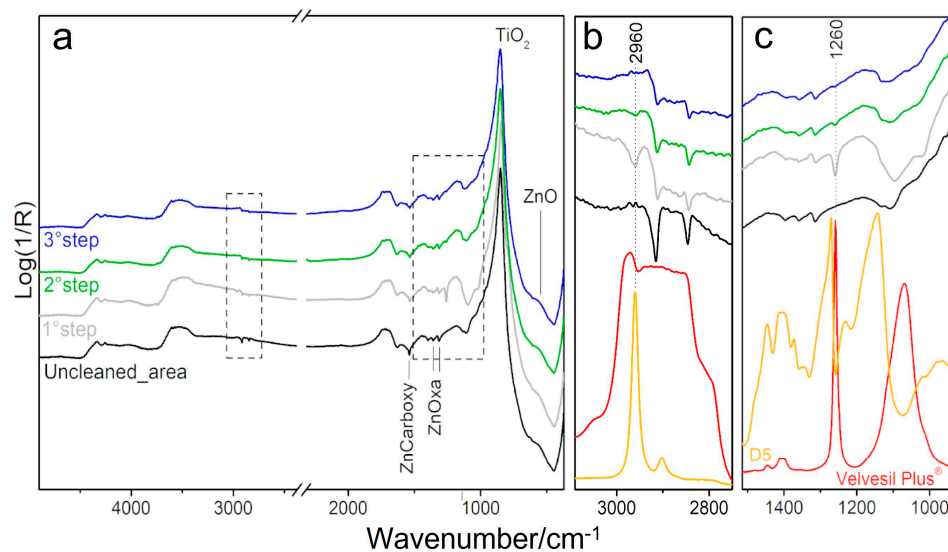


**Figure 5.** (a) ER-FTIR spectra collected on area P2 before cleaning (black profile), after dry removal of the silicone polymer emulsion (gray profile), and after the first and second rinsing steps with cyclomethicone D5 (green and blue profiles, respectively); (b,c) Enlarged views of the spectral ranges indicated by dashed boxes in (a) with the addition of the reference IR spectra of Velvesil Plus® (orange profile, transmission mode) and cyclomethicone D5 (green profile, reflection mode). ZnCarboxy = zinc carboxylate marker bands; ZnOxa = zinc oxalate marker bands.

#### 4. Discussion

A comparative analysis integrating both NMR  $T_2$  relaxation and FTIR spectroscopy data provides a clear hierarchy of performance among the four cleaning systems used on the surface of *Superficie 553*. The cleaning system, P2, composed of the buffer solution emulsified in the silicone polymer gel (VelvesilPlus®), was demonstrably the most invasive; it was the only method to leave detectable chemical residues on the surface, requiring multiple solvent rinses for removal. Furthermore, it uniquely induced a permanent and substantial “rigidification” of the paint’s molecular structure, as revealed by the NMR data. The other three systems (P1, P3, and P4) were chemically safe, with FTIR confirming the absence of residues and alterations to the paint’s constituent molecules. However, the NMR data indicated that both P1 (free buffer solution) and P4 (VanzanNF-C®) caused structural changes by permanently increasing the surface’s molecular mobility, converting a portion of the rigid matrix into a more flexible state.

This identifies the agar stick, used on area P3, as the optimal choice for this application. The NMR data for P3 showed only negligible changes in molecular mobility and structural distribution, indicating that the gel successfully controlled the cleaning action without causing plasticizing effects. This, combined with the FTIR confirmation of its chemical integrity and lack of residues, distinguishes P3 as the safest and most conservative cleaning method, achieving the goal of cleaning while best preserving the original physical and chemical state of the artwork.

#### 5. Conclusions

The combined use of portable NMR and FTIR constitutes a fundamental shift in the evaluation of conservation treatments, moving the decision-making process from a mostly aesthetic judgment to one grounded in objective scientific data. This synergistic approach

provides a comprehensive understanding of the impact of the cleaning system, something that the restorer's eye alone cannot perceive.

NMR spectroscopy acts as a powerful probe into the physical structure and molecular dynamics of the paint layers. It penetrates beyond the surface to answer critical questions: Has the cleaning agent caused hidden swelling or plasticization? Has it leached essential components, leading to embrittlement? Has it permanently altered the polymer network? As demonstrated in this study, a cleaning treatment that appears successful visually might have induced lasting changes in molecular mobility, such as the rigidification caused by system P2 or the increased flexibility observed in systems used in P1 and P4.

In parallel, FTIR spectroscopy provides the essential chemical composition analysis. It offers a chemical fingerprint, confirming that the original paint binder remains intact and, crucially, detecting the presence of any harmful residues left behind—a risk clearly identified with the P2 system. Furthermore, it validates the cleaning's effectiveness by demonstrating the removal of surface dirt while confirming that integral components have been preserved.

Ultimately, this dual-technique approach enables conservators to base their choices on robust experimental parameters. It allows them to select a method, like the P3 (Agar) system in this case, that is proven to be effective not only in its cleaning action but also non-invasive on both a physical and chemical level. This ensures the selection of the safer treatment for the long-term preservation of the artwork, transforming the evaluation of a cleaning test from a subjective art into an objective science.

**Author Contributions:** Conceptualization: V.D.T.; Methodology: N.P., P.M., E.M., P.C., D.D.L. and V.D.T.; Investigation: E.M., P.M., N.P. and V.D.T.; Resources: V.D.T., C.M., D.D.L. and P.C.; Data curation: N.P. and P.M.; Validation: V.D.T. and P.M.; Formal analysis and Visualization: N.P. and P.M.; writing—original draft preparation, V.D.T.; writing, review & editing: all the authors; Supervision: V.D.T.; Project administration: D.D.L., P.C. and C.M. All authors have read and agreed to the published version of the manuscript.

**Funding:** The diagnostic campaign was performed in 2018–2019 and was supported in part by MIUR through the National Access call (E-RISH.it, <https://www.e-rihs.eu/>) within the European Research Infrastructure for Heritage Science funded by the European Commission (H2020 INFRADEV-2016-2, GA n. 739503) and by the funding FOE MUR E-RIHS.

**Data Availability Statement:** The data presented in this study are available on request from the corresponding author.

**Acknowledgments:** The authors acknowledge all the institutions and scientists involved in this interdisciplinary project. In particular, we thank Cristiana Collu and the National Gallery of Modern and Contemporary Art (Rome) for hosting all the project partners. The authors are grateful to Guglielmo Capogrossi Guarna, President of the Fondazione Archivio Capogrossi, Rome, for his support of the research. Finally, Laura Baratin, President of the School of Conservation and Restoration of Cultural Heritage of the University of Urbino “Carlo Bo”, is gratefully acknowledged for making the research project possible.

**Conflicts of Interest:** The authors declare no conflicts of interest.

## Abbreviations

The following abbreviations are used in this manuscript:

NMR	Nuclear magnetic resonance
FTIR	Fourier Transform Infrared spectroscopy
BS	Buffer solution

## References

1. Banti, D.; La Nasa, J.; Tenorio, A.L.; Modugno, F.; van den Berg, K.J.; Lee, J.; Ormsby, B.; Burnstock, A.; Bonaduce, I. A molecular study of modern oil paintings: Investigating the role of dicarboxylic acids in the water sensitivity of modern oil paints. *RSC Adv.* **2018**, *8*, 6001–6012.
2. Lee, D.S.H.; Kim, N.S.; Scharff, M.; Nielsen, A.V.; Mecklenburg, M.; Fuster-López, L.; Bratasz, L.; Andersen, C.K. Numerical modelling of mechanical degradation of canvas paintings under desiccation. *Herit. Sci.* **2022**, *10*, 130. <https://doi.org/10.1186/s40494-022-00763-w>.
3. Silvester, G.; Burnstock, A.; Megens, L.; Learner, T.; Chiari, G.; van den Berg, K.J. A cause of water-sensitivity in modern oil paint films: The formation of magnesium sulphate. *Stud. Conserv.* **2014**, *59*, 38–51.
4. Harrison, J.; Lee, J.; Ormsby, B.; Payne, D.J. The influence of light and relative humidity on the formation of epsomite in cadmium yellow and French ultramarine modern oil paints. *Herit. Sci.* **2021**, *9*, 107. <https://doi.org/10.1186/s40494-021-00569-2>.
5. Tarilonte, E.; González-Mendia, O.; Costantini, I.; Castro, K.; Maguregui, I. A multi-analytical approach for the identification of surface whitening phenomena in contemporary oil painting and its application to metal soaps. *J. Cult. Herit.* **2025**, *74*, 195–203. <https://doi.org/10.1016/J.CULHER.2025.06.007>.
6. Chen-Wiegart, Y.C.K.; Catalano, J.; Williams, G.J.; Murphy, A.; Yao, Y.; Zumbulyadis, N.; Centeno, S.A.; Dybowski, C.; Thieme, J. Elemental and Molecular Segregation in Oil Paintings due to Lead Soap Degradation. *Sci. Rep.* **2017**, *7*, 11656. <https://doi.org/10.1038/s41598-017-11525-1>.
7. Eumelen, G.J.A.M.; Bosco, E.; Suiker, A.S.J.; Hermans, J.J. Chemo-mechanical model for degradation of oil paintings by amorphous and crystalline metal soaps. *Eur. J. Mech.-A/Solids* **2023**, *97*, 104827. <https://doi.org/10.1016/j.euromechsol.2022.104827>.
8. Cotte, M.; Checroun, E.; De Nolf, W.; Taniguchi, Y.; De Viguerie, L.; Burghammer, M.; Susini, J. Lead soaps in paintings: Friends or foes? *Stud. Conserv.* **2016**, *62*, 2–23. <https://doi.org/10.1080/00393630.2016.1232529>.
9. Hermans, J.J.; Keune, K.; van Loon, A.; Iedema, P.D. Toward a Complete Molecular Model for the Formation of Metal Soaps in Oil Paints. In *Metal Soaps in Art: Conservation and Research*; Springer: Cham, Switzerland, 2019. [https://doi.org/10.1007/978-3-319-90617-1\\_3](https://doi.org/10.1007/978-3-319-90617-1_3).
10. Baij, L.; Hermans, J.J.; Keune, K.; Iedema, P. Time-Dependent ATR-FTIR Spectroscopic Studies on Fatty Acid Diffusion and the Formation of Metal Soaps in Oil Paint Model Systems. *Angew. Chem. Int. Ed.* **2018**, *57*, 7351–7354. <https://doi.org/10.1002/anie.201712751>.
11. Casadio, F.; Keune, K.; Noble, P.; van Loon, A.; Hendriks, E.; Centeno, S.; Osmond, G. *Metal Soaps in Art: Conservation and Research*; Springer: Cham, Switzerland, 2019.
12. La Nasa, J.; Moretti, P.; Maniccia, E.; Pizzimenti, S.; Colombini, M.P.; Miliari, C.; Modugno, F.; Carnazza, P.; De Luca, D. Discovering Giuseppe Capogrossi: Study of the Painting Materials in Three Works of Art Stored at Galleria Nazionale (Rome). *Heritage* **2020**, *3*, 965–984. <https://doi.org/10.3390/heritage3030052>.
13. Wolbers, R. *Cleaning Painted Surfaces: Aqueous Methods*; Archetype Publications: London, UK, 2000.
14. Bandelli, D.; Mastrangelo, R.; Poggi, G.; Chelazzi, D.; Baglioni, P. New sustainable polymers and oligomers for Cultural Heritage conservation. *Chem. Sci.* **2024**, *15*, 2443–2455. <https://doi.org/10.1039/d3sc03909a>.
15. Chelazzi, D.; Baglioni, P. From Nanoparticles to Gels: A Breakthrough in Art Conservation Science. *Langmuir* **2023**, *39*, 10744–10755. <https://doi.org/10.1021/acs.langmuir.3c01324>.
16. Lagalante, A.F.; Wolbers, R.; Lagalante, A.F. The cleaning of acrylic paintings: New particle-based water-in-oil emulsifiers. In *Dall'Olio All'Acrilico, Dall'Impressionismo All'Arte Contemporanea*; Il Prato: Padova, Italy, 2016; pp. 107–114.
17. Cardaba, I.; Poggi, G.; Baglioni, M.; Chelazzi, D.; Maguregui, I.; Giorgi, R. Assessment of aqueous cleaning of acrylic paints using innovative cryogels. *Microchem. J.* **2020**, *152*, 104311. <https://doi.org/10.1016/j.microc.2019.104311>.
18. Albano, M.; Grassi, S.; Fiocco, G.; Invernizzi, C.; Rovetta, T.; Licchelli, M.; Marotti, R.; Merlo, C.; Comelli, D.; Malagodi, M. A preliminary spectroscopic approach to evaluate the effectiveness of water-and silicone-based cleaning methods on historical varnished brass. *Appl. Sci.* **2020**, *10*, 3982. <https://doi.org/10.3390/app10113982>.
19. Guilminot, E. The Use of Hydrogels in the Treatment of Metal Cultural Heritage Objects. *Gels* **2023**, *9*, 191. <https://doi.org/10.3390/gels9030191>.
20. Berrett, K.; Naude, V.; Wolbers, R. A new method for cleaning marble. *J. Am. Inst. Conserv.* **2007**, *14*, 197–211.
21. Liu, C.; Alvarez-Martin, A.; Keune, K. Exploring Benzyl Alcohol Derivatives and Related Compounds in the Cleaning of Oil Paintings. *Stud. Conserv.* **2024**, *69*, 348–359. <https://doi.org/10.1080/00393630.2023.2233374>.

22. Bertasa, M.; Botteon, A.; Brambilla, L.; Riedo, C.; Chiantore, O.; Poli, T.; Sansonetti, A.; Scaralone, D. Cleaning materials: A compositional multi-analytical characterization of commercial agar powders. *J. Anal. Appl. Pyrolysis* **2017**, *125*, 310–317. <https://doi.org/10.1016/j.jaap.2017.03.011>.
23. Sansonetti, A.; Bertasa, M.; Canevali, C.; Rabbolini, A.; Anzani, M.; Scaralone, D. A review in using agar gels for cleaning art surfaces. *J. Cult. Herit.* **2020**, *44*, 285–296.
24. Giordano, A.; Cremonesi, P. New methods of applying rigid agar gels: From tiny to large-scale surface areas. *Stud. Conserv.* **2021**, *66*, 437–448.
25. Bertasa, M.; Dodero, A.; Alloisio, M.; Vicini, S.; Riedo, C.; Sansonetti, A.; Scaralone, D.; Castellano, M. Agar gel strength: A correlation study between chemical composition and rheological properties. *Eur. Polym. J.* **2020**, *123*, 109442. <https://doi.org/10.1016/j.eurpolymj.2019.109442>.
26. Bosch-Roig, P.; Allegue, H.; Bosch, I. Granite pavement nitrate desalination: Traditional methods vs. biocleaning methods. *Sustainability* **2019**, *11*, 4227. <https://doi.org/10.3390/su11154227>.
27. Bosch-Roig, P.; Lustrato, G.; Zanardini, E.; Ranalli, G. Biocleaning of Cultural Heritage stone surfaces and frescoes: Which delivery system can be the most appropriate? *Ann. Microbiol.* **2014**, *65*, 1227–1241. <https://doi.org/10.1007/s13213-014-0938-4>.
28. Giordano, A.; Caruso, M.R.; Lazzara, G. New tool for sustainable treatments: Agar spray—Research and practice. *Herit. Sci.* **2022**, *10*, 123. <https://doi.org/10.1186/s40494-022-00756-9>.
29. Gulotta, D.; Saviello, D.; Gherardi, F.; Toniolo, L.; Anzani, M.; Rabbolini, A.; Goidanich, S. Setup of a sustainable indoor cleaning methodology for the sculpted stone surfaces of the Duomo of Milan. *Herit. Sci.* **2014**, *2*, 6. <https://doi.org/10.1186/2050-7445-2-6>.
30. Bertasa, M.; Poli, T.; Riedo, C.; Di Tullio, V.; Capitani, D.; Proietti, N.; Canevali, C.; Sansonetti, A.; Scaralone, D. A study of non-bounded/bounded water and water mobility in different agar gels. *Microchem. J.* **2018**, *139*, 306–314.
31. Busse, F.; Rehorn, C.; Küppers, M.; Ruiz, N.; Stege, H.; Blümich, B. NMR relaxometry of oil paint binders. *Magn. Reson. Chem.* **2020**, *58*, 830–839. <https://doi.org/10.1002/mrc.5020>.
32. Spyros, A.; Anglos, D. Study of Aging in Oil Paintings by 1D and 2D NMR Spectroscopy. *Anal. Chem.* **2004**, *76*, 4929–4936. <https://doi.org/10.1021/ac049350k>.
33. Wagner, N.; Catalano, J.; Di Tullio, V.; Pigliapochi, R.; Zumbulyadis, N.; Centeno, S.A.; Dybowski, C. Applications of NMR spectroscopy in cultural heritage science. In *Comprehensive Inorganic Chemistry III*; Elsevier: Amsterdam, The Netherlands, 2023; pp. 788–836. <https://doi.org/10.1016/B978-0-12-823144-9.00064-9>.
34. Nardelli, F.; Martini, F.; Lee, J.; Lluvears-Tenorio, A.; La Nasa, J.; Duce, C.; Ormsby, B.; Geppi, M.; Bonaduce, I. The stability of paintings and the molecular structure of the oil paint polymeric network. *Sci. Rep.* **2021**, *11*, 14202. <https://doi.org/10.1038/s41598-021-93268-8>. PMID: 34244532; PMCID: PMC8270892.
35. Blümich, B.; Perlo, J.; Casanova, F. Mobile single-sided NMR. *Prog. Nucl. Magn. Reson. Spectrosc.* **2008**, *52*, 197–269.
36. Eidmann, G.; Savelsberg, R.; Blümmler, P.; Blümich, B. The NMR MOUSE, a Mobile Universal Surface Explorer. *J. Magn. Reson. Ser. A* **1996**, *122*, 104–109. ISSN 1064-1858.
37. Perlo, J.; Casanova, F.; Blümich, B. Profiles with microscopic resolution by single-sided NMR. *J. Magn. Reson.* **2005**, *176*, 64–70.
38. Presciutti, F.; Perlo, J.; Casanova, F.; Glöggler, S.; Miliani, C.; Blümich, B.; Brunetti, B.G.; Sgamellotti, A. Non-invasive nuclear magnetic resonance profiling of painting layers. *Appl. Phys. Lett.* **2008**, *93*, 033505.
39. Gerony, F.; Thillaye du Boullay, C.; de Viguerie, L.; Michot, L.; Martinetto, P.; Le Denic, M.; Brageu, R.; Guillou, T.; Rollet, A.L.; Mériduet, G.; et al. Tempera paint solidification followed by single-sided NMR: An egg-cellent article that will dry you up. *Prog. Org. Coat.* **2025**, *208*, 109466. <https://doi.org/10.1016/j.porgcoat.2025.109466>.
40. Udell, N.A.; Hodgkins, R.E.; Berrie, B.H.; Meldrum, T. Physical and chemical properties of traditional and water-mixable oil paints assessed using single-sided NMR. *Microchem. J.* **2017**, *133*, 31–36. <https://doi.org/10.1016/j.microc.2017.03.013>.
41. Kiple, L.; Lee, T.; Zavaglia, G.; Meldrum, T. Characterization of molecular environments and chemical exchange in acrylic paints via single-sided NMR. *Prog. Org. Coat.* **2023**, *183*, 107770. <https://doi.org/10.1016/j.porgcoat.2023.107770>.
42. Di Tullio, V.; Zumbulyadis, N.; Centeno, S.A.; Catalano, J.; Wagner, M.; Dybowski, C. Water Diffusion and Transport in Oil Paints as Studied by Unilateral NMR and <sup>1</sup>H High-Resolution MAS-NMR Spectroscopy. *ChemPhysChem* **2020**, *21*, 113–119. <https://doi.org/10.1002/cphc.201900858>.
43. Di Tullio, V.; Pigliapochi, R.; Zumbulyadis, N.; Centeno, S.A.; Catalano, J.; Wagner, M.; Dybowski, C. Dynamics of diffusion, evaporation, and retention of organic solvents in paints by unilateral NMR and HR-MAS NMR spectroscopy. *Microchem. J.* **2023**, *190*, 108582. <https://doi.org/10.1016/j.microc.2023.108582>.

44. Gerony, F.; Fanost, A.; Tan, Z.R.; Malikova, N.; Michot, L.; Poirier-Quinot, M.; de Viguerie, L.; Jaber, M.; Mériguet, G.; Rollet, A.L. Structural and dynamical impacts of water dilution on egg yolk properties. *Soft Matter* **2025**, *23*, 4666–4680. <https://doi.org/10.1039/D5SM00289C>.
45. Angelova, L.V.; Ormsby, B.; Richardson, E. Diffusion of water from a range of conservation treatment gels into paint films studied by unilateral NMR. Part I: Acrylic emulsion paint. *Microchem. J.* **2016**, *124*, 311–320. <https://doi.org/10.1016/j.microc.2015.09.012>.
46. Di Tullio, V.; Sciutto, G.; Proietti, N.; Prati, S.; Mazzeo, R.; Colombo, C.; Cantisani, E.; Romè, V.; Rigaglia, D.; Capitani, D. <sup>1</sup>H NMR depth profiles combined with portable and micro-analytical techniques for evaluating cleaning methods and identifying original, non-original, and degraded materials of a 16th century Italian wall painting. *Microchem. J.* **2018**, *141*, 40–50.
47. Carretti, E.; Rosi, F.; Miliani, C.; Dei, L. Monitoring of Pictorial Surfaces by mid-FTIR Reflectance Spectroscopy: Evaluation of the Performance of Innovative Colloidal Cleaning Agents. *Spectrosc. Lett.* **2005**, *38*, 459–475.
48. Moretti, P.; Rosi, F.; Miliani, C.; Daugherty, M.; Jan van den Berg, K.; Cartechini, L. Non-invasive reflection FT-IR spectroscopy for on-site detection of cleaning system residues on polychrome surfaces. *Microchem. J.* **2020**, *157*, 105033.

**Disclaimer/Publisher's Note:** The statements, opinions and data contained in all publications are solely those of the individual author(s) and contributor(s) and not of MDPI and/or the editor(s). MDPI and/or the editor(s) disclaim responsibility for any injury to people or property resulting from any ideas, methods, instructions or products referred to in the content.